Hindawi
Complexity
Volume 2018, Article ID 5754908, 12 pages
https://doi.org/10.1155/2018/5754908

Research Article

A Hybrid Tabu Search Algorithm for a Real-World Open Vehicle Routing Problem Involving Fuel Consumption Constraints

Yunyun Niu,[1] **Zehua Yang**,[1] **Ping Chen**,[2] **and Jianhua Xiao**[3]

[1] *School of Information Engineering, China University of Geosciences, Beijing, Beijing 100083, China*
[2] *School of Business, Nankai University, Tianjin 300071, China*
[3] *The Research Center of Logistics, Nankai University, Tianjin 300071, China*

Correspondence should be addressed to Jianhua Xiao; jhxiao2008@163.com

Received 4 October 2017; Accepted 1 February 2018; Published 28 February 2018

Academic Editor: Danilo Comminiello

Outsourcing logistics operation to third-party logistics has attracted more attention in the past several years. However, very few papers analyzed fuel consumption model in the context of outsourcing logistics. This problem involves more complexity than traditional open vehicle routing problem (OVRP), because the calculation of fuel emissions depends on many factors, such as the speed of vehicles, the road angle, the total load, the engine friction, and the engine displacement. Our paper proposed a green open vehicle routing problem (GOVRP) model with fuel consumption constraints for outsourcing logistics operations. Moreover, a hybrid tabu search algorithm was presented to deal with this problem. Experiments were conducted on instances based on realistic road data of Beijing, China, considering that outsourcing logistics plays an increasingly important role in China's freight transportation. Open routes were compared with closed routes through statistical analysis of the cost components. Compared with closed routes, open routes reduce the total cost by 18.5% with the fuel emissions cost down by nearly 29.1% and the diver cost down by 13.8%. The effect of different vehicle types was also studied. Over all the 60- and 120-node instances, the mean total cost by using the light-duty vehicles is the lowest.

1. Introduction

Many developing countries are confronted with two problems: how to reduce economic costs and how to develop an environment-friendly society. As a result, researchers as well as companies with integrated logistics expertise tend to adopt new transportation models to counter these problems. Outsourcing logistics operations to the third-party logistics would reduce costs through better resource utilization and operations efficiency in freight transportation. It plays an increasingly important role in freight transportation. In that case, a company can hire vehicles from other companies to deliver its goods. Vehicles do not need return to the company as usual. They are usually described as the open vehicle routing problem (OVRP) [1]. Compared with the vehicle routing problem (VRP), routes in the OVRP model are open; see Figure 1.

The OVRP is NP-hard [2], so heuristics or metaheuristics methods are usually used to deal with it [3], such as the tabu search [4], the neighborhood-based search [5], particle swarm optimization [6], ant colony optimization [7], or evolutionary computing [8]. Hybrid metaheuristic algorithms were also designed to solve the OVRP [9]. Moreover, several variants of the OVRP were studied to model specific practical problems. OVRP with time windows (OVRPTW) was presented by [10] to model the delivery of multiproduct newspapers. The multidepot OVRP (MDOVRP) was first proposed by [11] to model the distribution of fresh meat. The open vehicle routing problem with decoupling points (OVRP-DP) was introduced in [12] to describe open routes performed by more than one carrier. The OVRP with uncertain demands was investigated to deal with nondeterministic customer demands and avoid unsatisfied demands or more extra operation cost [13]. However, among models studied in the past there are rare formulations considering the impact of fuel and carbon emission [14]. This paper is a contribution to this line of research.

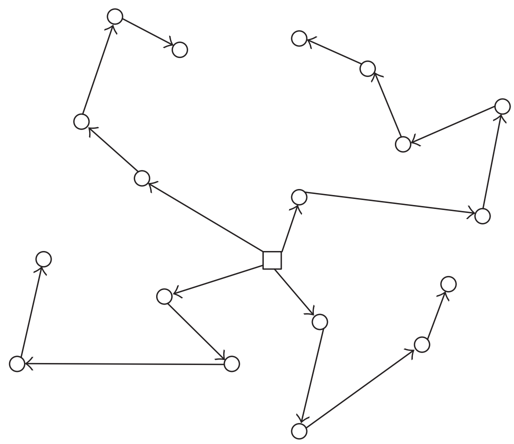

Figure 1: Open vehicle routing problem.

Carbon emissions along with freight transportation have hazardous impacts on the environment. How to minimize the fuel consumption becomes a hot topic. In [15], six fuel consumption models were compared with each other and several factors affecting carbon emissions in road transportation were analyzed. In [16], the pollution-routing problem (PRP) was introduced to evaluate the greenhouse gas emissions for the VRP. The total energy consumed on each road can be directly translated into greenhouse gas emissions with the PRP model. Reference [17] considered a heterogeneous vehicle fleet and extended the PRP model. Reference [18] presented a recent review of studies on green freight transportation problems.

This study has been motivated by a real problem in Beijing, China. As outsourcing logistics is playing a more and more important role in China's freight transportation, many companies hire vehicles from the third-party logistics. Vehicles do not need return to the depot after delivering products to customers. Each route departs from the depot and ends up with one of the customers. These companies are facing the problem of minimizing the total cost, including both fuel consumption cost and driver salaries.

The main contributions of our paper are summarized as follows. (1) Fuel consumption was analyzed in the context of the OVRP; and the green open vehicle routing problem (GOVRP) model was constructed. With the purpose of optimizing the fuel emissions cost in the model, we introduced the comprehensive modal emission model (CMEM) into the OVRP model and extend the OVRP with an objective that accounts for the amount of greenhouse emissions. (2) A hybrid tabu search algorithm involving several neighborhood search strategies was proposed to solve the GOVRP. A modified nearest neighborhood heuristic (mNNH) was proposed to get the initial solution. It considered two factors load and distance when searching for a suitable initial solution. And then four neighborhood search operators were designed to produce the neighborhood of the current solution. (3) Computational experiments were conducted on instances derived from real geographical data of customers in Beijing, China. Both the effect of open routes and the effect of vehicle types were analyzed in respects of reducing total cost.

2. Mathematical Model of the GOVRP

The CMEM was developed by [19, 20] to calculate fuel emissions. In this section, we introduced the CMEM to the OVRP and formulated the mathematical model of the GOVRP. The fuel consumption F^h (in liters) of vehicle type h is given by [21]

$$F^h = \lambda\left(\frac{k^h N^h V^h d}{v} + M^h \gamma^h \alpha d + \beta^h \gamma^h d v^2\right), \qquad (1)$$

where $\lambda = \xi/\kappa\psi$, $\gamma^h = 1/1000 n_{tf}\eta$, $\alpha = \tau + g\sin\theta + gC_r^h\cos\theta$, and $\beta^h = 0.5C_d A^h \rho$ are constraints. M^h is the total vehicle weight, d is the distance, and v is the vehicle speed. Three terms of F^h are referred to as the engine module, the weight module, and the speed module, respectively. Notations and their default values are listed in the following two tables [17, 22]. Common parameters of vehicles are listed in Table 1. Specific parameters for different vehicle types are listed in Table 2.

Let $N = \{0, \ldots, n\}$ be the set of customers and the depot, and let $A = \{(i, j) : i, j \in N,\ i \neq j,\ j \neq 0\}$ be the set of arcs. Node 0 denotes the depot, so the customer set is $N_0 = N \setminus \{0\}$. Q represents the capacity of vehicles. Variables q_i means the demand of customer i. Variables d_{ij} is the distance from node i to node j. Variables f_{ij} are the total amount of flow on arc (i, j). The mathematical model of GOVRP is defined as follows:

$$\text{Minimize} \quad \sum_{(i,j)\in A} \lambda f_c k N V d_{ij} \sum_{r=1}^{R} \frac{z_{ij}^r}{v^r} \qquad (2)$$

$$+ \sum_{(i,j)\in A} \lambda f_c \gamma \alpha_{ij} d_{ij} \left(w x_{ij} + f_{ij}\right) \qquad (3)$$

$$+ \sum_{(i,j)\in A} \lambda f_c \beta \gamma d_{ij} \sum_{r=1}^{R} \left(v^r\right)^2 z_{ij}^r \qquad (4)$$

$$+ \sum_{j\in N_0} f_d s_j \qquad (5)$$

$$\text{subject to} \quad \sum_{j\in N_0} x_{0j} \leq \left|N_0\right| \qquad (6)$$

$$\sum_{i\in N} x_{ij} = 1, \quad \forall j \in N_0 \qquad (7)$$

$$\sum_{j\in N} x_{ij} \leq 1, \quad \forall i \in N_0 \qquad (8)$$

$$\sum_{i=1}^{n} x_{i0} = 0 \qquad (9)$$

$$q_j x_{ij} \leq f_{ij} \leq \left(Q - q_i\right) x_{ij}, \quad \forall (i, j) \in A \qquad (10)$$

$$\sum_{j\in N} f_{ij} - \sum_{j\in N} f_{ji} = q_i, \quad \forall i \in N_0 \qquad (11)$$

$$\sum_{r=1}^{R} z_{ij}^r = x_{ij}, \quad \forall (i, j) \in A \qquad (12)$$

Table 1: Common parameters of vehicles.

Notation	Description	Typical values
ξ	Fuel-to-air mass ratio	1
g	Gravitational constant (m/s^2)	9.81
ρ	Air density (kg/m^3)	1.2041
C_r^h	Coefficient of rolling resistance	0.01
η	Efficiency parameter for diesel engines	0.45
f_c	Fuel and CO_2 emissions cost (RMB/liter)	12.0165
f_d	Driver wage (RMB/s)	0.0111
κ	Heating value of a typical diesel fuel (kj/g)	44
ψ	Conversion factor (g/s to L/s)	737
n_{tf}	Vehicle drive train efficiency	0.45
v^l	Lower speed limit (m/s)	0
v^u	Upper speed limit (m/s)	27.8 (or 100 km/h)
τ	Acceleration (m/s^2)	0

Table 2: Specific parameters for different vehicle types.

Notation	Description	Light duty	Medium duty	Heavy duty
w	Curb weight (kg)	3500	5500	14,000
Q	Maximum payload (kg)	4000	12,500	26,000
k	Engine friction factor (kj/rev/liter)	0.25	0.20	0.15
N	Engine speed (rev/s)	38.34	36.67	30.0
V	Engine displacement (liter)	4.5	6.9	10.5
C_d	Coefficient of aerodynamics drag	0.6	0.7	0.9
A	Frontal surface area (m^2)	7.0	8.0	10.0

$$x_{ij} \in \{0,1\}, \quad \forall (i,j) \in A \tag{13}$$

$$z_{ij}^r \in \{0,1\}, \quad \forall (i,j) \in A \tag{14}$$

$$f_{ij} \geq 0, \quad \forall (i,j) \in A. \tag{15}$$

Formula (2)–(5) describes the objective of the GOVRP, where terms (2)–(4) calculate the total fuel consumption cost and term (5) measures the total driver wages. More specifically, f_c is the fuel emissions cost per liter, and terms (2)–(4) calculate the fuel consumption costs induced by the engine module, the weight module, and the speed module, respectively. s_j denotes the total time spent on a route where j is the last served customer.

The binary variable x_{ij} is equal to 1 if there is a vehicle traveling on arc (i, j); otherwise, x_{ij} is equal to 0. Constraints (6)–(9) ensure that each customer is served by one vehicle and it is served only once. Vehicles do not return to the deport. If i is the last served customer, constraint (8) can be written as $\sum_{j\in N} x_{ij} = 0$. Otherwise, it can be written as $\sum_{j\in N} x_{ij} = 1$. Constraints (10) and (11) define flows. The binary variable z_{ij}^r is equal to 1 when a vehicle travels on arc (i, j) at speed v^r.

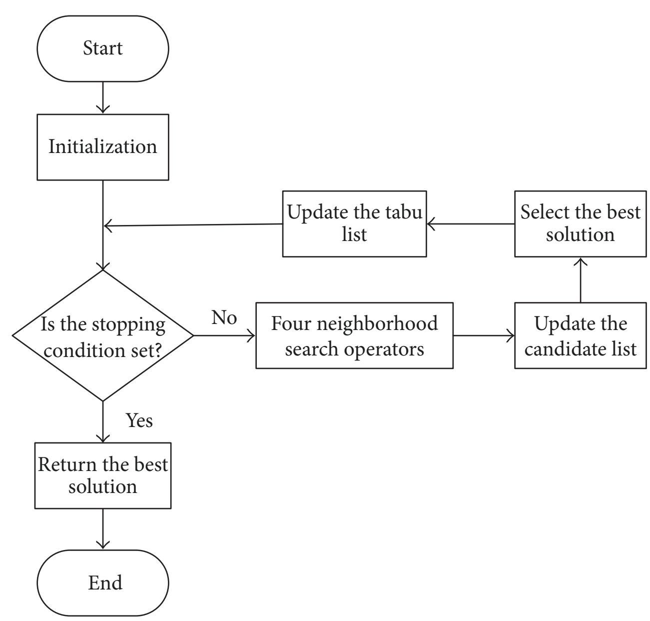

Figure 2: The flowchart of our algorithm.

3. Hybrid Tabu Search Algorithm for the GOVRP

In this study, a hybrid tabu search algorithm including several neighborhood search strategies was designed to solve the GOVRP. The flowchart of this algorithm is shown in Figure 2. The detailed steps are listed as follows.

Step 1. The initial setup includes initializing an empty tabu list and an empty candidate list, creating an initial solution, setting that initial solution as the best solution to date. A modified nearest neighborhood heuristic (mNNH) is used to gain the initial solution. We will elaborate on it specifically in Section 3.1.

Step 2. If the stopping condition is satisfied, the search process stops, and the best solution is returned. Otherwise, it turns to Step 3.

Step 3. The solution space is explored each step from a current solution to the accepted solutions in the neighborhood by using four efficient neighborhood search algorithms. For each neighbor of the current solution X_{current}, the optimal speed on each arc of their routes is set by using the speed optimization algorithm according to [23].

Step 4. The neighboring solutions are checked for tabu elements. We search for the best solution and update the candidate list.

Step 5. If the best local candidate is better than the current best solution, update the current best solution. The local optimal solution is added to the tabu list. Then, turn to Step 2.

In this paper, the stopping condition is the maximum number of iterations $X_{\max}$. When our algorithm is iterated $X_{\max}$ times, the algorithm is terminated.

3.1. The Initial Solution. We use a modified nearest neighborhood heuristic (mNNH) to obtain an initial solution. The mNNH considers two factors load and distance when searching for a suitable initial solution. In a delivery system, a vehicle can reduce q_j load after servicing customer j. We define

$$\overline{\Delta f_{ij}} = \frac{q_j}{d_{ij}}, \quad i \in N,\ j \in N_{\text{ucs}}, \tag{16}$$

where N_{unc} is defined as the unrouted customer set.

The mNNH builds routes one by one according to the following steps. The first route begins with an unrouted customer r, which can be calculated by the following equation:

$$r = \arg\max_{j \in N_{\text{ucs}}} \left\{ \left| \overline{\Delta f_{0j}} \right| \right\}. \tag{17}$$

Then, we calculate $\overline{\Delta f_{ij}}$ between the current node r and the other unrouted nodes. We choose the node with the greatest current $\overline{\Delta f_{ij}}$ value as the next node if the current route does not violate the vehicle capacity constraint. We update the current node r and search for the next node in the same way. When no customer can be assigned to the route, a new route is started. When all the customers are already routed, the process stops. The algorithm is described as Algorithm 1.

3.2. The Neighborhood Search. The neighborhood of the current solution X_{current} is first obtained by four neighborhood search operators. They cannot violate the capacity constraint during this process as before. Then, the optimal speed on each route is set according to [23].

Input: $Q, q_1, \ldots, q_n$
Output: *path*
Set $N_{\text{ucs}} = \{1, \ldots, n\}$, $path = \emptyset$, $route = \emptyset$
while $N_{\text{ucs}} \neq \emptyset$ **do**
  Select a car
  Set $q \leftarrow Q$
  while $q - q_j \geq 0$ and $N_{\text{ucs}} \neq \emptyset$ **do**
    Set $route \leftarrow route \cup \{r\}$, $q \leftarrow q - q_j$, $i \leftarrow j$
    $N_{\text{ucs}} \leftarrow N_{\text{ucs}}/\{j\}$, $r \leftarrow \arg\max_{j \in N_{\text{ucs}}}\{|\overline{\Delta f_{ij}}|\}$
  Set $path \leftarrow path \cup \{route\}$, $route = \emptyset$
return *path*

Algorithm 1: A modified nearest neighborhood heuristic.

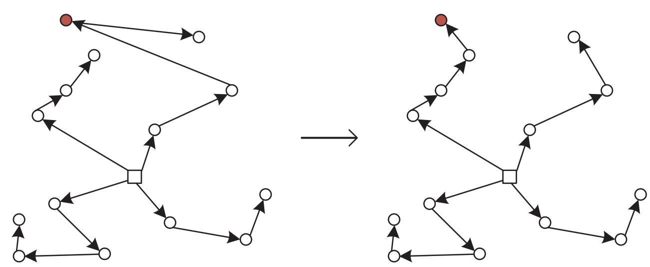

Figure 3: High-cost-node improvement operator.

Table 3: Algorithmic parameters values.

Notation	Description	Typical values
$X_{\max}$	The maximum iteration number	500
l_t	The length of Tabu list	5
n_1	The number of RO in each step	40
n_2	The number of HCNIO in each step	5
l	The threshold in SRIO in each step	3
p	Each route has a chance p to be improved	50%

(1) Random Operator (RO). It randomly selects one node from the solution and then randomly finds a possible position for it.

(2) High-Cost-Node Improvement Operator (HCNIO). As illustrated in Figure 3, the operator tries to reassign the high cost node u^*, because the total distance between its preceding customer and its following customer is the longest. Customer u^* can be calculated as follows:

$$u^* = \arg\max_{u \in N} \left\{ d_{iu} + d_{uj} \right\}, \tag{18}$$

where i is the preceding customer and j is the following customer.

We compute the best possible position for node u based on

$$c\left(i^*, u, j^*\right) = \min\left[c\left(i, u, j\right)\right], \quad i, j \in N,\ i, j \neq N_{\text{ucs}}, \tag{19}$$

Table 4: Cost components with Min TC.

Instances	TD (m)	ET (s)	FEC (RMB)	DC (RMB)	TC (RMB)	CE (kg)
BJ10_01	160000	1.52	641.04	1427.23	2068.27	123.77
BJ10_02	215400	1.21	860	1669.73	2529.73	166.04
BJ10_03	148200	1.43	598.82	1515.92	2114.74	115.61
BJ10_04	125700	1.32	512.95	1604.03	2116.98	99.03
BJ10_05	131600	1.39	527.49	1261.2	1788.69	101.84
BJ10_06	195700	1.28	800.49	1731.86	2532.35	154.55
BJ10_07	161200	1.51	629.72	1462.42	2092.15	121.58
BJ10_08	160500	1.46	643.06	1598.9	2241.96	124.15
BJ10_09	174300	1.29	708.01	1687.92	2395.93	136.69
BJ10_10	196900	1.32	794.67	1724.37	2519.03	153.42
BJ20_01	207050	1.78	847.71	2872.04	3719.75	163.67
BJ20_02	327870	1.89	1313.52	3411.58	4725.1	253.6
BJ20_03	214080	1.84	869.09	2954.44	3823.52	167.79
BJ20_04	255540	2.01	1012	2740.72	3752.73	195.39
BJ20_05	276920	1.88	1118.67	3355.55	4474.22	215.98
BJ20_06	289340	2.18	1144.59	3143.29	4287.89	220.98
BJ20_07	303290	1.74	1257.06	3656.81	4913.87	242.7
BJ20_08	272120	1.8	1118.93	2995.08	4114.01	216.03
BJ20_09	310000	1.93	1250.4	3023.52	4273.93	241.41
BJ20_10	273670	2.25	1086.06	2945.31	4031.37	209.68
BJ30_01	383030	2.52	1594.7	4489.58	6084.28	307.89
BJ30_02	413850	2.62	1653.91	4497.14	6151.06	319.32
BJ30_03	425160	2.27	1763.89	4932.42	6696.31	340.55
BJ30_04	422810	2.55	1735.05	4702.76	6437.8	334.98
BJ30_05	348850	2.82	1405.68	4627.92	6033.6	271.39
BJ30_06	459680	2.28	1907.54	4772.35	6679.89	368.28
BJ30_07	460900	2.51	1900.86	4826.39	6727.26	367
BJ30_08	423510	2.38	1742.33	4625.07	6367.4	336.39
BJ30_09	447060	2.35	1869.31	4768.26	6637.57	360.9
BJ30_10	281950	2.59	1141.17	4007.94	5149.11	220.32

where $c(i,u,j) = d_{iu} + d_{uj} - d_{ij}$ is the cost for inserting node u between customer i and customer j and $\overline{N_{\text{ucs}}} \subseteq N$ is the set of currently routed customers.

(3) Short-Route Improvement Operator (SRIO). The operator tries to combine or delete short routes by reassigning nodes belonging to those routes. A threshold l is set to evaluate the length of a route. Only if the length of a route is shorter than the threshold l, the nodes in that route can be reassigned to other positions. The process can be illustrated in Figure 4 ($l = 2$). First, arcs in the shorter routes are deleted and then isolated nodes are assigned to other longer routes.

The best possible position for each unrouted node u is also calculated by (19). By using (20), the most suitable customer is selected to be inserted in the route repeatedly. Unrouted nodes will be inserted to the current routes one by one.

$$c'(i^*, u^*, j^*) = \min\left[c(i^*, u, j^*)\right]. \tag{20}$$

(4) Random-Route-Improvement Operator (RRIO). Each route in the current solution has a chance p of being destroyed. In that case, customers in that route should be reassigned. The best possible position for each node u is calculated by (19). Then best customer to be inserted in the route is selected by using (20) repeatedly. All other unrouted customers will be inserted into the sequence one by one. As shown in Figure 5, two routes included in the dotted oval are destroyed; nodes in those routes are reassigned in possible positions.

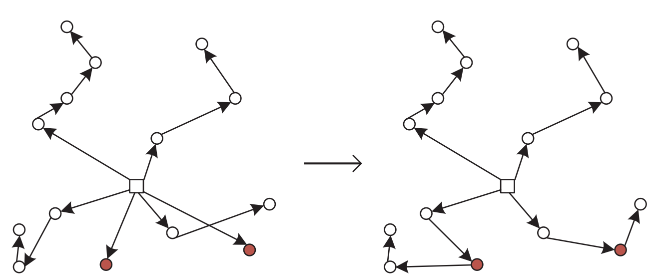

Figure 4: Short-route improvement operator.

Table 5: Cost components with Min FEC.

Instances	TD (m)	ET (s)	FEC (RMB)	DC (RMB)	TC (RMB)	CE (kg)
BJ10_01	160000	1.5	641.04	1427.23	2068.27	123.77
BJ10_02	215400	1.21	860	1669.73	2529.73	166.04
BJ10_03	148200	1.56	598.82	1515.92	2114.74	115.61
BJ10_04	126500	1.37	511.94	1607.36	2119.3	98.84
BJ10_05	132750	1.47	519.04	1265.98	1785.02	100.21
BJ10_06	195500	1.31	800.42	1731.02	2531.45	154.54
BJ10_07	161200	1.57	629.72	1462.42	2092.15	121.58
BJ10_08	161900	1.5	640.76	1604.72	2245.47	123.71
BJ10_09	174300	1.3	708.01	1687.92	2395.93	136.69
BJ10_10	196900	1.33	794.67	1724.37	2519.03	153.42
BJ20_01	207400	1.76	849.35	2873.49	3722.84	163.98
BJ20_02	328330	1.95	1309.37	3413.49	4722.86	252.8
BJ20_03	214900	1.97	872.32	2957.85	3830.17	168.42
BJ20_04	255610	2.18	1011.35	2741.01	3752.36	195.26
BJ20_05	277600	1.94	1120.84	3358.38	4479.21	216.4
BJ20_06	289930	2.25	1139.38	3145.75	4285.12	219.98
BJ20_07	304560	1.79	1262.84	3662.1	4924.93	243.81
BJ20_08	273430	1.88	1118.78	3000.53	4119.3	216
BJ20_09	309870	2.04	1247.69	3022.98	4270.67	240.89
BJ20_10	273750	2.25	1082.62	2945.65	4028.27	209.02
BJ30_01	382650	2.42	1589.04	4488	6077.04	306.79
BJ30_02	413260	2.74	1652.82	4494.69	6147.51	319.11
BJ30_03	421230	2.27	1747.69	4916.08	6663.77	337.42
BJ30_04	422830	2.43	1736.24	4702.84	6439.08	335.21
BJ30_05	352760	2.75	1417.82	4644.18	6062	273.74
BJ30_06	458930	2.19	1903.61	4769.23	6672.84	367.53
BJ30_07	458810	2.49	1884.59	4817.7	6702.3	363.86
BJ30_08	426290	2.32	1748.32	4636.63	6384.94	337.54
BJ30_09	452450	2.3	1890.76	4790.68	6681.44	365.05
BJ30_10	281430	2.6	1135.95	4005.78	5141.73	219.32

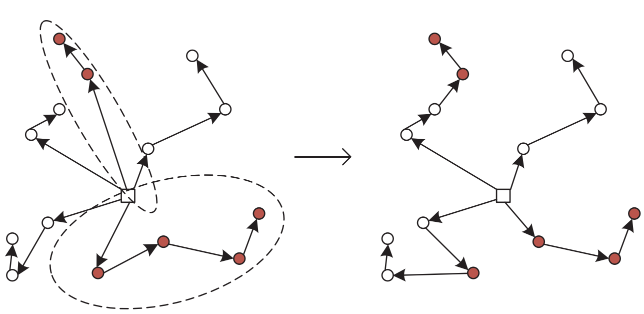

Figure 5: Random-route-improvement operator.

For each neighbor of the current solution X_{current}, the optimal speed on each route is set. According to [23], the optimal speed is

$$v^* = \left(\frac{kNV}{2\beta\gamma} + \frac{f_d}{2\beta\gamma f_c}\right)^{1/3}. \quad (21)$$

4. Computational Analysis

Experiments are run with data derived from real geographical distances of customers in Beijing. Three smaller classes with 10, 20, and 30 customers and four larger classes with 60, 80, 100, and 120 customers are generated. Each class includes 10 instances. All the customers involved in this study are shown in Figure 6. The algorithmic parameters values are given in Table 3.

4.1. Effect of Objectives Min TD, Min FEC and Min DC. Three different objectives, Min TD (total distance), Min FEC (fuel emissions cost), and Min DC (driver cost), are used to minimize the total distance, fuel emissions cost, and driver cost, respectively. We obtained solutions with different cost components on each performance measure and analyzed the effect of different objectives. Experiments were conducted on 10-, 20-, and 30-node instances by using light-duty vehicles. The mean result of each instance collected over ten runs is reported; see Tables 4, 5, and 6. The columns display total distance (TD), execution time (ET), fuel emissions cost

Table 6: Cost component with Min DC.

Instances	TD (m)	ET (s)	FEC (RMB)	DC (RMB)	TC (RMB)	CE (kg)
BJ10_01	159400	1.44	644.62	1424.74	2069.36	124.46
BJ10_02	215400	1.21	860	1669.73	2529.73	166.04
BJ10_03	148200	1.47	598.82	1515.92	2114.74	115.61
BJ10_04	125200	1.39	518.15	1601.95	2120.11	100.04
BJ10_05	131600	1.39	530.81	1261.2	1792	102.48
BJ10_06	195620	1.3	800.46	1731.52	2531.99	154.54
BJ10_07	161200	1.45	629.72	1462.42	2092.15	121.58
BJ10_08	160400	1.48	646.39	1598.48	2244.87	124.8
BJ10_09	174300	1.29	709.63	1687.92	2397.55	137.01
BJ10_10	196900	1.32	794.67	1724.37	2519.03	153.42
BJ20_01	206800	1.74	846.78	2871	3717.78	163.49
BJ20_02	329150	1.82	1327.82	3416.9	4744.72	256.36
BJ20_03	215720	1.81	879.27	2961.26	3840.53	169.76
BJ20_04	256490	1.99	1018.96	2744.67	3763.63	196.73
BJ20_05	280140	1.85	1134.25	3368.94	4503.19	218.99
BJ20_06	292080	2.1	1158.64	3154.69	4313.33	223.7
BJ20_07	303580	1.7	1259.44	3658.02	4917.46	243.16
BJ20_08	272670	1.78	1123.32	2997.37	4120.69	216.88
BJ20_09	310710	1.89	1254.84	3026.47	4281.31	242.27
BJ20_10	271600	2.18	1076.31	2936.7	4013.01	207.8
BJ30_01	381430	2.35	1589.86	4482.93	6072.79	306.95
BJ30_02	420450	2.47	1689.85	4524.59	6214.44	326.26
BJ30_03	427000	2.15	1773.68	4940.07	6713.75	342.44
BJ30_04	422740	2.35	1748.59	4702.47	6451.05	337.6
BJ30_05	352590	2.57	1423.67	4643.47	6067.14	274.87
BJ30_06	458020	2.17	1904.47	4765.45	6669.91	367.69
BJ30_07	459540	2.33	1897.68	4820.74	6718.42	366.38
BJ30_08	430970	2.21	1784.59	4656.09	6440.68	344.55
BJ30_09	445190	2.18	1864.22	4760.49	6624.71	359.92
BJ30_10	282940	2.44	1146.82	4012.06	5158.88	221.42

Table 7: Cost components with different objectives.

Instances	Objective	TD (m)	ET (s)	FEC (RMB)	DC (RMB)	TC (RMB)	CE (kg)
10-node	Min FEC	167265	1.41	670.44	1569.67	2240.11	129.44
	Min DC	166822	1.37	673.33	1567.83	2241.15	130
	Min TC	166950	1.37	671.63	1568.36	2239.98	129.67
20-node	Min FEC	273538	2	1101.45	3112.12	4213.57	212.66
	Min DC	273894	1.89	1107.96	3113.6	4221.57	213.91
	Min TC	272988	1.93	1101.8	3109.83	4211.64	212.72
30-node	Min FEC	407064	2.45	1670.68	4626.58	6297.27	322.56
	Min DC	408087	2.32	1682.34	4630.84	6313.18	324.81
	Min TC	406680	2.49	1671.44	4624.98	6296.43	322.7

(FEC), driver cost (DC), total cost (TC), and CO_2 emissions (CE). Table 7 presents the average results of each class.

On average of 10-node class, the fuel emissions cost represents about 30% of the total cost. For 20- and 30-node classes, the fuel emissions cost accounts for approximately 26% of the total cost. The carbon dioxide emissions increase with the number of customers. Only considering the driver cost in the objective leads to the most carbon dioxide emissions and the poorest total cost performance. Only considering the fuel emissions gets solutions with the lowest carbon dioxide emissions, but a higher total cost. Min TC as an objective yields the lowest total cost and the shortest total distance.

Table 8: Cost components with closed routes.

Instances	TD (m)	ET (s)	FEC (RMB)	DC (RMB)	TC (RMB)	CE (kg)
BJ10_01	243300	1.35	973.42	1773.67	2747.08	187.94
BJ10_02	287900	1.23	1143.69	1971.25	3114.95	220.81
BJ10_03	233000	1.28	929.49	1868.6	2798.09	179.46
BJ10_04	193600	1.33	774.88	1886.42	2661.31	149.61
BJ10_05	190300	1.33	752.29	1505.32	2257.61	145.24
BJ10_06	306900	1.26	1216.62	2194.33	3410.94	234.89
BJ10_07	225500	1.19	914.3	1729.84	2644.14	176.52
BJ10_08	222400	1.33	883.91	1856.33	2740.24	170.65
BJ10_09	250200	1.29	1001.88	2003.58	3005.46	193.43
BJ10_10	285200	1.3	1133.7	2091.6	3225.3	218.88
BJ20_01	296880	1.75	1191.94	3245.63	4437.57	230.13
BJ20_02	432490	1.74	1733.98	3846.68	5580.66	334.78
BJ20_03	302470	1.93	1227.85	3322.04	4549.9	237.06
BJ20_04	350360	1.8	1408.36	3135.07	4543.43	271.91
BJ20_05	397350	1.75	1601.07	3856.4	5457.48	309.12
BJ20_06	404900	1.76	1627.02	3623.9	5250.92	314.13
BJ20_07	453910	1.79	1833.88	4283.23	6117.1	354.06
BJ20_08	377970	1.71	1526.82	3435.3	4962.12	294.78
BJ20_09	458430	1.79	1842.5	3640.83	5483.32	355.73
BJ20_10	380810	1.75	1533.55	3390.9	4924.45	296.08
BJ30_01	544130	2.53	2213.58	5159.58	7373.16	427.37
BJ30_02	602750	2.32	2434.58	5282.76	7717.34	470.04
BJ30_03	603420	2.25	2446.55	5673.79	8120.33	472.35
BJ30_04	574210	2.51	2328.31	5332.41	7660.72	449.52
BJ30_05	495510	2.46	2006.16	5237.86	7244.02	387.33
BJ30_06	636960	2.23	2584.8	5509.64	8094.44	499.04
BJ30_07	666890	2.43	2711.67	5683.09	8394.76	523.54
BJ30_08	588990	2.25	2385.82	5313.28	7699.1	460.63
BJ30_09	640480	2.22	2600.55	5572.68	8173.23	502.08
BJ30_10	394830	2.35	1599.07	4477.4	6076.47	308.73

Table 9: Cost components of different types of routes.

Instances	Type of routes	TD (m)	ET (s)	FEC (RMB)	DC (RMB)	TC (RMB)	CE (kg)
10-node	Open	166950	1.37	671.63	1568.36	2239.98	129.67
	Closed	243830	1.29	972.42	1888.09	2860.51	187.74
20-node	Open	272988	1.93	1101.8	3109.83	4211.64	212.72
	Closed	385557	1.78	1552.7	3578	5130.7	299.78
30-node	Open	406680	2.49	1671.44	4624.98	6296.43	322.7
	Closed	574817	2.36	2331.11	5324.25	7655.36	450.06

4.2. Effect of Open Routes. In this subsection, we compared the total cost of open routes with that of closed routes. Experiments were also conducted on smaller instance classes by using light-duty vehicles. The mean results of closed routes collected over ten runs are listed in Table 8. The average results of each class are reported in Table 9 to illustrate the effect of open routes. As shown in Table 9, open routes reduce the total cost by 18.5% with the fuel emissions cost down by nearly 29.1% and the diver cost down by 13.8% over all the instances.

4.3. Results for Larger Scale Instances. Experiments were also conducted on the four largest sets with the objective Min TC. The results collected over ten runs are reported in Table 10 by using light-duty vehicles. Notations BS, MS, WS, SD, and ET in columns represent the best solution, mean solution,

Table 10: Computational results on larger scale instances.

Instance	BS (RMB)	MS (RMB)	WS (RMB)	SD	ET (s)
BJ60_01	11061.79	11254.42	11417.58	92.8	5.37
BJ60_02	10309.83	10393.21	10492.87	62.43	4.88
BJ60_03	11574.38	11790.03	11933.82	94.03	5.06
BJ60_04	12094.39	12212.64	12462.25	95.54	5.14
BJ60_05	11236.35	11320.09	11431.91	52.74	5.44
BJ60_06	11883.87	12040.48	12249.58	94.39	4.89
BJ60_07	12600.43	12745.03	12867.3	92.99	4.74
BJ60_08	11939.78	12060.86	12173.83	59.37	4.73
BJ60_09	11583.85	11727.88	11922.82	95.35	4.7
BJ60_10	12938.11	13121.2	13364.03	114.64	4.74
BJ80_01	14787.03	15036.55	15227.3	127.09	7.56
BJ80_02	14018.34	14220.78	14411.5	115.1	7.18
BJ80_03	14714.36	14964.93	15139.74	125.11	7.72
BJ80_04	13872.84	14065.74	14550.33	199.54	7.6
BJ80_05	14613.9	14788.56	15078.73	148.41	7.52
BJ80_06	16857.87	17148.49	17572.08	217.41	6.83
BJ80_07	15371.73	15632.16	15925.82	170.46	7.1
BJ80_08	14273.97	14484.07	14815.66	183.64	7.39
BJ80_09	14526.1	14743.32	14969.09	122.54	7.19
BJ80_10	14736.48	14942.92	15284.86	137.4	7.09
BJ100_01	19330.25	19617.94	20069.92	203.78	10.22
BJ100_02	20194.9	20701.34	21013.24	215.65	10.33
BJ100_03	20081.75	20286.97	20556.28	138.13	10.38
BJ100_04	18483.02	18689.28	18893.14	114.28	9.87
BJ100_05	18776.99	18983.5	19256.85	165.22	10.01
BJ100_06	17478.28	17764.38	18119.14	187.27	10.5
BJ100_07	18451.61	18775.37	18938.18	167.43	10.49
BJ100_08	18527.85	18762.86	18941.62	142.11	10.52
BJ100_09	17458.07	18048.33	18385.66	259.49	10.92
BJ100_10	20847	21099.27	21541.13	201.04	10
BJ120_01	21699.63	21954.27	22209.26	135.47	15.38
BJ120_02	22803.9	23135.32	23736.67	273.1	16.09
BJ120_03	22074.76	22569.41	22921.39	270.03	17.46
BJ120_04	22380.9	22560.26	22764.57	138.1	16.91
BJ120_05	22602.33	23308.71	23666.93	289.5	14.39
BJ120_06	22656.5	22975.25	23166.4	145.56	14.44
BJ120_07	21156.14	21711.99	22170.6	301.69	14.37
BJ120_08	20837.63	21069.17	21418.09	211.61	15.66
BJ120_09	21865.67	22195.93	22498.88	170.26	14.43
BJ120_10	22705.98	23054.33	23556.8	217.54	14.4

the worst solution, standard deviation, and execution time, respectively. As shown in Table 10, the total cost increases with the number of customers.

4.4. Results with Different Vehicle Types. Experiments were conducted on the 60- and 120-node instances by using different types of vehicles. In this subsection, the analysis focuses on which type of vehicle is the most suitable to minimize the total cost. The specific vehicle parameters are listed in Table 2. Results with different vehicle types are listed in Tables 11 and 12. Over all the instances in the two classes, the mean total cost by using the light-duty vehicles is the lowest. For 120-node instances, the mean total cost by using medium-duty vehicles increases by 4.8% and the result by using heavy-duty vehicles rises 23.6%. For 60-node instances, the mean total cost by using medium-duty vehicles increases by 7.7% and the value by using heavy-duty vehicles rises 28%.

Table 11: Computational results on the 60-node instances by using different vehicles.

Type of vehicles	Instance	BS (RMB)	MS (RMB)	WS (RMB)	SD	ET (s)
Only light duty	BJ60_01	11061.79	11254.42	11417.58	92.8	5.37
	BJ60_02	10309.83	10393.21	10492.87	62.43	4.88
	BJ60_03	11574.38	11790.03	11933.82	94.03	5.06
	BJ60_04	12094.39	12212.64	12462.25	95.54	5.14
	BJ60_05	11236.35	11320.09	11431.91	52.74	5.44
	BJ60_06	11883.87	12040.48	12249.58	94.39	4.89
	BJ60_07	12600.43	12745.03	12867.3	92.99	4.74
	BJ60_08	11939.78	12060.86	12173.83	59.37	4.73
	BJ60_09	11583.85	11727.88	11922.82	95.35	4.7
	BJ60_10	12938.11	13121.2	13364.03	114.64	4.74
Only medium duty	BJ60_01	12449.13	12616.53	12823.93	109.15	4.51
	BJ60_02	11328.74	11557.08	11780.96	125.14	4.19
	BJ60_03	12959.56	13222.5	13390.12	121.83	4.42
	BJ60_04	13411.61	13630.23	13870.71	147.61	4.4
	BJ60_05	12515.46	12678.95	12843.89	87.75	4.63
	BJ60_06	13037.75	13302.09	13413.95	100.83	4.29
	BJ60_07	12360.13	12425.3	12579.82	63.71	4.22
	BJ60_08	12942.29	13064.34	13360.38	121.13	4.49
	BJ60_09	12112.23	12348.68	12563.22	122.72	4.43
	BJ60_10	12832.96	12974.52	13105.98	88.75	4.03
Only heavy duty	BJ60_01	14787.24	14995.59	15334.52	176.58	9.38
	BJ60_02	13418.08	13700.42	13911.3	143.14	7.91
	BJ60_03	15469.9	15746.78	16052.25	183.26	7.54
	BJ60_04	16164.2	16411.77	16729.41	172.11	7.78
	BJ60_05	14772.72	14937.7	15269.37	154.91	7.98
	BJ60_06	15893.22	16093.82	16272.75	133.43	7.41
	BJ60_07	14441.09	14606.23	14757.43	103.53	7.46
	BJ60_08	15088.73	15473.2	15638.19	152.24	7.61
	BJ60_09	14521.68	14811.72	14972.54	119.53	7.22
	BJ60_10	14961.08	15164.55	15321.96	109.22	6.88

Figure 6: Customer nodes.

5. Conclusions

In this study, the GOVRP was introduced as a formulation considering the impact of fuel emissions for the third-party logistics. The problem was to construct open routes for vehicles to visit all customers with the vehicle capacity constraints. The objective was to minimize the total cost composing of the fuel emissions cost and the driver cost.

A hybrid tabu search algorithm was designed to deal with the GOVRP instances. Experiments were conducted on 60 instances derived from real geographical data of customers in Beijing. We analyzed the cost components with different objectives and compared open routes with closed routes in respects of reducing the total cost. A homogenous fleet was considered in this paper. Computational results showed that vehicle type influenced the total cost and it should be changed

Table 12: Computational results on the 120-node instances by using different vehicles.

Type of vehicles	Instance	BS (RMB)	MS (RMB)	WS (RMB)	SD	ET (s)
Only light duty	BJ120_01	21699.63	21954.27	22209.26	135.47	15.38
	BJ120_02	22803.9	23135.32	23736.67	273.1	16.09
	BJ120_03	22074.76	22569.41	22921.39	270.03	17.46
	BJ120_04	22380.9	22560.26	22764.57	138.1	16.91
	BJ120_05	22602.33	23308.71	23666.93	289.5	14.39
	BJ120_06	22656.5	22975.25	23166.4	145.56	14.44
	BJ120_07	21156.14	21711.99	22170.6	301.69	14.37
	BJ120_08	20837.63	21069.17	21418.09	211.61	15.66
	BJ120_09	21865.67	22195.93	22498.88	170.26	14.43
	BJ120_10	22705.98	23054.33	23556.8	217.54	14.4
Only medium duty	BJ120_01	23290.23	23541.68	23691.38	124.27	12.99
	BJ120_02	23133.82	23473.76	23710.98	178.16	12.55
	BJ120_03	23320.12	23573.14	23908.95	186.7	12.9
	BJ120_04	23117.27	23545.71	23757.64	194.07	13.01
	BJ120_05	23687.6	24099.96	24385.48	207.61	13.08
	BJ120_06	23273.19	23621.69	23870.13	162.68	12.49
	BJ120_07	23136.08	23257.6	23424.7	91.21	13.13
	BJ120_08	22752.22	23085.88	23320.75	200.2	13.35
	BJ120_09	23171.61	23279.47	23450.24	85.55	12.65
	BJ120_10	23476.59	23845.67	24258.76	222.02	12.58
Only heavy duty	BJ120_01	27565.54	27974.16	28341.07	204.51	20.49
	BJ120_02	27337.33	27628.98	28138.69	243.32	18.79
	BJ120_03	26855.88	27379.48	27991.72	327.29	20.89
	BJ120_04	27580.86	27834.25	28040.53	168.47	21.69
	BJ120_05	28189.69	28500.43	28755.03	186.67	18.96
	BJ120_06	27679.42	27933.79	28172.32	143.93	19.15
	BJ120_07	26969.4	27668.76	28014.39	286.72	21.03
	BJ120_08	26617.8	27268.75	27742.87	315.44	22.64
	BJ120_09	27000.07	27382.75	27631.08	187.61	20.21
	BJ120_10	27663.24	27887.53	28107.04	126.69	20.54

according to the instance's size. In the future, a heterogeneous fleet of vehicles can be used to minimize the total cost. Other types of the OVRP, such as OVRPTW and MDOVRP, can be solved by our algorithm with some changes.

Nowadays, several novel computing techniques are used to deal with complex problems. Some of them are bioinspired models, such as membrane-inspired evolutionary algorithms [24–26] and probe machine [27]. Their nondeterministic distributed parallel frameworks have been proved to improve the performance of optimization algorithms [28]. Most of them can be used to solve real-life problems [29]. We hope that more competitive results for our GOVRP instances can be obtained by using those algorithms in the future.

Conflicts of Interest

The authors declare that they have no conflicts of interest.

Acknowledgments

This work was supported by the National Natural Science Foundation of China (Grant nos. 61502012, 61772290, and 61373066); the Beijing Natural Science Foundation (Grant no. 4164096); the Humanity and Social Science Youth Foundation of Ministry of Education of China (Grant no. 13YJC630010); the Science and Technology Development Strategy Research Program of Tianjin (Grant no. 16ZLZXZF00030); and the Collaborative Innovation Center for China Economy.

References

[1] L. Schrage, "Formulation and structure of more complex/realistic routing and scheduling problems," *Networks*, vol. 11, no. 2, pp. 229–232, 1981.

[2] S. Raff, "Routing and scheduling of vehicles and crews: the state of the art," *Computers and Operations Research*, vol. 10, no. 2, pp. 63–211, 1983.

[3] J. Brandao, "A tabu search algorithm for the open vehicle routing problem," *European Journal of Operational Research*, vol. 157, no. 3, pp. 552–564, 2004.

[4] U. Derigs and K. Reuter, "A simple and efficient tabu search heuristic for solving the open vehicle routing problem," *Journal of the Operational Research Society*, vol. 60, no. 12, pp. 1658–1669, 2009.

[5] E. E. Zachariadis and C. T. Kiranoudis, "An open vehicle routing problem metaheuristic for examining wide solution neighborhoods," *Computers and Operations Research*, vol. 37, no. 4, pp. 712–723, 2010.

[6] S. A. Mirhassani and N. Abolghasemi, "A particle swarm optimization algorithm for open vehicle routing problem," *Expert Systems with Applications*, vol. 38, no. 9, pp. 11547–11551, 2011.

[7] X.-Y. Li, P. Tian, and S. C. H. Leung, "An ant colony optimization metaheuristic hybridized with tabu search for open vehicle routing problems," *Journal of the Operational Research Society*, vol. 60, no. 7, pp. 1012–1025, 2009.

[8] S. Yu, C. Ding, and K. Zhu, "A hybrid GA-TS algorithm for open vehicle routing optimization of coal mines material," *Expert Systems with Applications*, vol. 38, no. 8, pp. 10568–10573, 2011.

[9] P. P. Repoussis, C. D. Tarantilis, O. Braysy, and G. Ioannou, "A hybrid evolution strategy for the open vehicle routing problem," *Computers and Operations Research*, vol. 37, no. 3, pp. 443–455, 2010.

[10] R. Russell, W.-C. Chiang, and D. Zepeda, "Integrating multi-product production and distribution in newspaper logistics," *Computers & Operations Research*, vol. 35, no. 5, pp. 1576–1588, 2008.

[11] C. D. Tarantilis and C. T. Kiranoudis, "Distribution of fresh meat," *Journal of Food Engineering*, vol. 51, no. 1, pp. 85–91, 2002.

[12] R. Atefi, M. Salari, L. C. Coelho, and J. Renaud, "The open vehicle routing problem with decoupling points," *European Journal of Operational Research*, vol. 265, no. 1, pp. 316–327, 2018.

[13] C. Erbao, L. Mingyong, and Y. Hongming, "Open vehicle routing problem with demand uncertainty and its robust strategies," *Expert Systems with Applications*, vol. 41, no. 7, pp. 3569–3575, 2014.

[14] K. Fleszar, I. H. Osman, and K. S. Hindi, "A variable neighbourhood search algorithm for the open vehicle routing problem," *European Journal of Operational Research*, vol. 195, no. 3, pp. 803–809, 2009.

[15] E. Demir, T. Bektaş, and G. Laporte, "A comparative analysis of several vehicle emission models for road freight transportation," *Transportation Research Part D: Transport and Environment*, vol. 16, no. 5, pp. 347–357, 2011.

[16] T. Bektaş and G. Laporte, "The pollution-routing problem," *Transportation Research Part B: Methodological*, vol. 45, no. 8, pp. 1232–1250, 2011.

[17] Ç. Koç, T. Bektaş, O. Jabali, and G. Laporte, "The fleet size and mix pollution-routing problem," *Transportation Research Part B: Methodological*, vol. 70, pp. 239–254, 2014.

[18] E. Demir, T. Bektaş, and G. Laporte, "A review of recent research on green road freight transportation," *European Journal of Operational Research*, vol. 237, no. 3, pp. 775–793, 2014.

[19] M. Barth, T. Younglove, and G. Scora, "Development of a Heavy-duty Diesel Modal Emissions and Fuel Consumption Model," Tech. Rep. UCB-ITSPRR-2005-1, California PATH Program, Institute of transportation Studies, University of California at Berkeley, California, Calif, USA, 2005.

[20] M. Scora and G. Barth, "Comprehensive Modal Emission Model (CMEM), Version 3.01, User Guide," Tech. Rep., 2006, http://www.cert.ucr.edu/cmem/docs/CMEM_User_Guide_v3.01d.pdf.

[21] M. Barth and K. Boriboonsomsin, "Real-world carbon dioxide impacts of traffic congestion," *Transportation Research Record*, no. 2058, pp. 163–171, 2008.

[22] Man, Trucks in Distribution Transport, http://www.mantruckandbus.co.uk/en/trucks/start_trucks.html.

[23] E. Demir, T. Bektas, and G. Laporte, "An adaptive large neighborhood search heuristic for the Pollution-Routing PROblem," *European Journal of Operational Research*, vol. 223, no. 2, pp. 346–359, 2012.

[24] G. Zhang, H. Rong, F. Neri, and M. J. Pérez-Jiménez, "An optimization spiking neural P system for approximately solving combinatorial optimization problems," *International Journal of Neural Systems*, vol. 24, no. 5, pp. 1–16, 2014.

[25] G. Zhang, H. Rong, J. Cheng, and Y. Qin, "A population-membrane-system-inspired evolutionary algorithm for distribution network reconfiguration," *Chinese Journal of Electronics*, vol. 23, no. 3, pp. 437–441, 2014.

[26] X. Zhang, J. Li, and L. Zhang, "A multi-objective membrane algorithm guided by the skin membrane," *Natural Computing*, vol. 15, no. 4, pp. 597–610, 2016.

[27] J. Xu, "Probe machine," *IEEE Transactions on Neural Networks and Learning Systems*, vol. 27, no. 7, pp. 1405–1416, 2016.

[28] G. Zhang, J. Cheng, M. Gheorghe, and Q. Meng, "A hybrid approach based on differential evolution and tissue membrane systems for solving constrained manufacturing parameter optimization problems," *Applied Soft Computing*, vol. 13, no. 3, pp. 1528–1542, 2013.

[29] G. Zhang, M. J. Prez-Jimnez, and M. Gheorghe, *Real-Life Applications with Membrane Computing*, Springer, Berlin, Germany, 2017.